EARTHQUAKE ENGINEERING AND STRUCTURAL DYNAMICS, VOL. 26, 409–422 (1997)

SLIDING MODE CONTROL OF BUILDINGS WITH ATMD

RAJESH ADHIKARI* AND HIROKI YAMAGUCHI†

Saitama University, Department of Civil and Environmental Engineering, 255 Shimo-Okubo, Urawa Saitama 338, Japan

SUMMARY

In the present paper, the application of the sliding mode control (SMC) scheme is discussed in a systematic manner for controlling the vibration of tall buildings with an Active Tuned Mass Damper (ATMD) installed at the top floor. It is shown that the application of the SMC theory for buildings with ATMD may lead to large responses in the building due to the interaction effect from the ATMD caused by the comparatively large response of the ATMD. Based on the theory of compensators, a method is proposed which eliminates the interaction effect from the ATMD to the building and thus prevents large response in the building. The results are demonstrated through simple numerical examples of building–ATMD system subjected to initial condition loading as well as two different types of external excitations. © 1997 by John Wiley & Sons, Ltd.

KEY WORDS: non-linear control; sliding mode control; building–ATMD system; compensator

INTRODUCTION

The control of the response of tall buildings subjected to uncertain dynamic loadings, such as wind load and earthquake load, has drawn the interest of many practical civil engineers. As a result, various control schemes—passive as well as active—have been developed to reduce the building vibrations. Among these two control schemes, active control scheme has recently emerged as a new structural control strategy. Among the various active control schemes which have caught the interest of civil engineers, e.g. active tendon control,[1–3] control by active appendages,[4,5] active tuned mass damper or ATMD,[3,5–8] etc., ATMD has been one of the most popular and the most widely accepted control devices. As a result of various research and technological developments in the field of active control, ATMD systems have even found a number of practical applications, though mostly in Japan.[7,8]

The design of an ATMD system has, so far, been based on the linear feedback control theories like pole allocation, LQ control theory and H^{∞} control theory. These feedback control theories essentially involve stationary eigenstructure assignment to the structure under some predefined excitation level or some required level of damping. Since both wind-induced vibrations and earthquake-induced ones are inherently non-stationary processes, the efficiency of the controllers obtained by assigning stationary eigenstructure to the structure could not be the best for the non-stationary vibration problems encountered in reality.

In contrast with the linear feedback control theories, non-linear control theories possess various merits which can make them a suitable choice for the control of vibration problems in the civil engineering field. The property of adaptiveness and robustness to the changes in the responses, imparted to the non-linear control schemes due to the non-linear control actions, makes them a superior choice over the linear feedback control schemes.[12,13,21] Several other arguments about suitability of the non-linear control over linear control scheme for the civil engineering control problems can be found in Bhartia *et al.*[9] In this paper, we choose a non-linear control scheme known as the Sliding Mode Control (SMC) which is known to be robust against variations in certain system parameters or external excitations.[10–16] Recently, with reference to the control of

* Research Associate
† Professor

CCC 0098–8847/97/040409–14$17·50

Received 26 October 1995
Revised 1 October 1996

the civil engineering structures, SMC has been studied by Yang *et al.*[17] also. It was shown by Adhikari and Yamaguchi[18] that a SMC-based robust-adaptive control scheme can be obtained by making the magnitude of non-linear control action a function of the uncertainty in the excitations. From a practical view point, it is desirable to extend the concept of SMC-based robust-adaptive control scheme to the control of building vibrations by using ATMD as a control device.

However, certain practical problems may arise with the direct application of the SMC theory for the control of tall buildings with ATMD. It is shown in this paper that, even with an optimally designed sliding surface,[19] large response of the ATMD can prevent the controlled system from reaching the sliding mode. This may lead to a large control force to be applied on the structure and thereby exciting the structure instead of controlling it. Therefore, we propose to use a filter, commonly also known as 'compensator',[20] to filter out the undesirable effects of the ATMD response on the control scheme. It is demonstrated through a simple example that the effects of the structure–ATMD interaction can be eliminated by the use of a properly designed compensator, which, thus, results in a better control scheme for SMC when applied to structures with ATMD as a control device.

PROBLEMS IN DIRECT APPLICATION OF SMC WITH ATMD

Formulation of the Sliding Mode Control (SMC)

In the SMC framework, a switching surface, known as the *sliding surface*, is first defined in the state space of the system. A non-linear switched feedback control law is then obtained which drives the trajectories of the controlled system onto this surface. The condition that the system trajectories stay on the sliding surface is known as the sliding mode.[10–16] Thus, the design of SMC involves two basic steps – design of a sliding surface and the design of a non-linear switched feedback control law. The concept of the sliding surface together with the sliding mode is schematically shown in Figure 1.

The non-linear control force in the SMC framework can be expressed as[13,15]

$$u(\mathbf{x}, t) = u_{eq}(\mathbf{x}, t) - \eta\,\mathrm{sgn}(\sigma(\mathbf{x})) \tag{1}$$

where u_{eq} is the linear part of the control force, known as the *equivalent control force*, η is a parameter which imparts discontinuity to the control action across the so-called *sliding surface* $\sigma(\mathbf{x})$ and sgn is the usual *signum* function, defined as $\mathrm{sgn}(\sigma(\mathbf{x})) = \sigma(\mathbf{x})/|\sigma(\mathbf{x})|$. The magnitude of η, and thus the non-linear control action, depends on the expected uncertainty in the external excitation or parameter variation.[13,21]

For an m-storey building model with an ATMD system installed at the top, as shown in Figure 2, the equation of motion can be written in the state-space form as

$$\dot{\mathbf{x}} = \mathbf{A}\mathbf{x} + \mathbf{B}u(t) + \mathbf{H}\mathbf{f}(t) \tag{2}$$

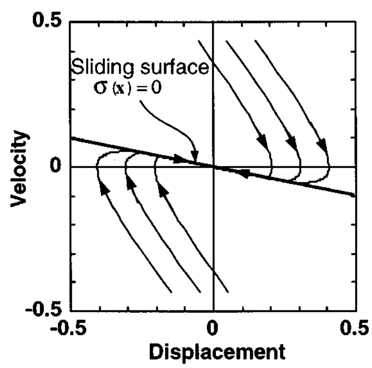

Figure 1. Concept of sliding surface and the sliding mode

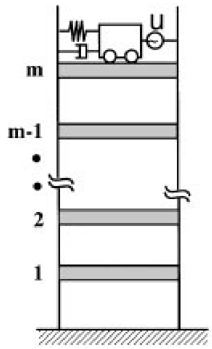

Figure 2. A model of a tall building with an ATMD at the top

where $\mathbf{x}$ is the state vector of size $2n$ (n being equal to $m+1$), $\mathbf{A}$ is a $2n \times 2n$ system matrix, $\mathbf{B}$ is the control force location vector of size $2n$, $\mathbf{H}$ is the external force location matrix of size $2n \times p$, $\mathbf{f}(t)$ is the external force vector of size p, and $u(t)$ is the scalar control input.

The equivalent control force u_{eq} is obtained by following the Utkin–Draženovic 'method of equivalent control',[11,16] which states that in the sliding mode the system satisfies $\sigma(\mathbf{x}) = 0$ and $\dot{\sigma}(\mathbf{x}) = 0$, and the control force is the so-called equivalent control force. For $\sigma(\mathbf{x}) = \mathbf{Sx}$, chosen to be linear function of the states of the system, satisfying $\dot{\sigma}(\mathbf{x}) = \mathbf{S}\dot{\mathbf{x}} = 0$, yields

$$u_{eq}(\mathbf{x}, t) = -(\mathbf{SB})^{-1}[\mathbf{SAx} + \mathbf{SHf}(t)] \tag{3}$$

where $|(\mathbf{SB})^{-1}| = 0$, and the sliding surface coefficient matrix $\mathbf{S}$ is a design matrix, usually constant, of size $r \times 2n$. Herein, r is the number of control inputs, which in the present case is equal to 1. The method of designing an optimal sliding surface coefficient matrix $\mathbf{S}$ is discussed in Utkin and Young.[19]

Clearly, the control law of equation (3) cannot be synthesized explicitly if the external excitation term $\mathbf{f}(t)$ is not known *a priori*, which is generally the case with the loading encountered with in the vibration problems related to civil engineering structures. However, under appropriate conditions, the control given in equation (3) can be synthesized implicitly via discontinuous (chattering) control defined in terms of the known system parameters. We, therefore, drop the term containing $\mathbf{f}(t)$ from equation (3) and, instead, through a properly selected value of η, impart a non- linear switching discontinuous control action to account for the uncertainty in the excitation. The choice of η and hence the control force $u(\mathbf{x}, t)$ must be such that the existence and the reachability of the sliding mode is guaranteed. Mathematically expressed, the condition that $\sigma(\mathbf{x})\,\dot{\sigma}(\mathbf{x}) < 0$, must be satisfied.[11,14,15] This results in

$$\eta(t) \geqslant |\mathbf{SB}^{-1}\mathbf{SH}\hat{\mathbf{f}}(t)| \tag{4}$$

where $\hat{\mathbf{f}}(t)$ is the total estimated uncertainty in the controlled system and it refers to the uncertainty in the system due to the error in the modelling of the system itself or it could refer to the uncertainty in the external excitations. In the present paper, we define $\hat{\mathbf{f}}(t)$ in terms of the uncertainty in the external excitation.

The realizable control force is, therefore, expressed as

$$u(\mathbf{x}, t) = -(\mathbf{SB})^{-1}\mathbf{SAx} - \eta(t)\,\mathrm{sgn}(\sigma(\mathbf{x})) \tag{5}$$

where $\eta(t)$ is obtained from equation (4). Note that $\mathbf{f}(t)$ of equation (3) has been neglected in equation (5).

The direct implementation of the control given by equation (5), however, results in the so-called *chattering* which is highly undesirable. Therefore, chattering is eliminated by smoothing the control force in a thin 'boundary layer' of thickness ε in the neighbourhood of $\sigma(\mathbf{x})$.[13] The control force devoiding the chattering condition, is thus obtained as

$$u(\mathbf{x}, t) = -(\mathbf{SB})^{-1}\mathbf{SAx} - \eta(t)\,\mathrm{sat}(\sigma(\mathbf{x})/\varepsilon) \tag{6}$$

where sat is a *saturation* function defined as

$$\operatorname{sat}(\sigma(\mathbf{x})/\varepsilon) = \begin{cases} \sigma(\mathbf{x})/\varepsilon & \text{if } |\sigma(\mathbf{x})/\varepsilon| \leqslant 1 \\ \operatorname{sgn}(\sigma(\mathbf{x})/\varepsilon) & \text{otherwise} \end{cases} \tag{7}$$

In all of the numerical examples presented in this paper, ε was assumed to be 0·001. Since, in practice, the actuators are always of limited capacity, following Yang *et al.*,[17] the following constraints are imposed on the force capacity of the actuator:

$$u(t) = \begin{cases} u(\mathbf{x}, t) & \text{when } |u(\mathbf{x}, t)| \leqslant u_{\mathrm{MAX}} \\ \dfrac{u(\mathbf{x}, t)}{|u(\mathbf{x}, t)|} u_{\mathrm{MAX}} & \text{when } |u(\mathbf{x}, t)| > u_{\mathrm{MAX}} \end{cases} \tag{8}$$

where u_{MAX} is the maximum force capacity of the actuator.

Numerical examples

The sliding mode control algorithm discussed above is applied to the control of a 100 m tall existing Huis Ten Bosch building at Nagasaki, Japan. The modal properties of this building as well as the response history of the building subjected to strong wind are available together with the time-history records of the wind velocity. Since the analysis of the response data showed that the first mode response was dominant, the building was modelled as a SDOF model for control. Two different control arrangements, as shown in Figure 3, are discussed herein. The first modal mass of the building is approximately equal to $698{\cdot}95 \times 10^3$ kg, the natural frequency and the structural damping of the building model are 0·625 Hz and 1 per cent, respectively. Figure 3(a) depicts the case of a SDOF model of the building under direct force control, whereas Figure 3(b) depicts the same building model with an ATMD installed at the top. We discuss both cases one by one in the following.

Example 1(a) (Figure 3(a)). Assuming the state vectors to be $\mathbf{x} = [x \ \dot{x}]^{\mathrm{T}}$, the system matrices for the building model shown in Figure 3(a) are obtained as

$$\mathbf{A} = \begin{bmatrix} 0 & 1 \\ -\omega^2 & -2\xi\omega \end{bmatrix}, \qquad \mathbf{B} = [0 \quad 1/M]^{\mathrm{T}} \quad \text{and} \quad \mathbf{H} = [0 \quad 1/M]^{\mathrm{T}}$$

where M is the modal mass of the first mode, ω and ξ are the first mode frequency and the structural damping, respectively.

Following the method discussed by Utkin and Young,[19] an optimal sliding surface was obtained by minimizing a quadratic performance index with the weighting matrix Q chosen as $Q = \operatorname{diag}[1 \ \ 5]$. The sliding surface coefficient matrix $\mathbf{S}$ was obtained to be $\mathbf{S} = [0{\cdot}4472 \ \ 1]$ and thus $\sigma(\mathbf{x}) = 0{\cdot}4472x + \dot{x}$.

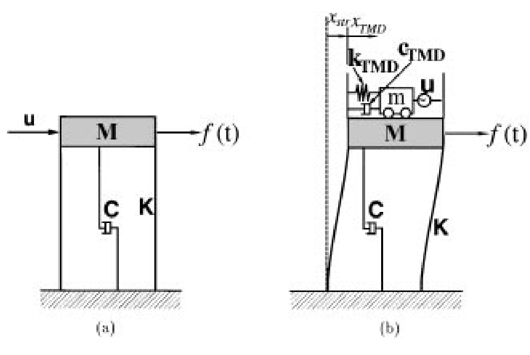

Figure 3. Example problems: (a) SDOF model of a tall building with force control; (b) SDOF model of a tall building with an ATMD at the top

The uncontrolled response of the building from an initial condition of $\mathbf{x}(0) = [0{\cdot}01 \quad 0{\cdot}01]$, is shown in Figure 4, whereas the controlled responses of the building are shown in Figures 5 and 6. Here, η was selected to be a constant equal to 10 kN. Figure 5 depicts the case for no constraint on the control force, whereas the maximum control force available was assumed to be 20 kN for the case of Figure 6. In Figure 5, the existence of the sliding surface is very clear and the control objective is completely achieved. However, when the control force has a limited capacity, as can be seen in Figure 6, the length of the sliding mode is considerably reduced. Nonetheless, in both of the cases the control objectives are achieved.

Example 1b (Figure 3b). Assuming the state vectors to be $\mathbf{x} = [x_S \ x_{TMD} \ \dot{x}_S \ \dot{x}_{TMD}]^T$, the system matrices for the building–ATMD model shown in Figure 3(b) are obtained to be

$$\mathbf{A} = \begin{bmatrix} 0 & 0 & 1 & 0 \\ 0 & 0 & 0 & 1 \\ -(\omega_S^2 + \mu\omega_{TMD}^2) & \mu\omega_{TMD}^2 & -2(\xi_S\omega_S + \mu\xi_{TMD}\omega_{TMD}) & 2\mu\xi_{TMD}\omega_{TMD} \\ \omega_S^2 & -\omega_{TMD}^2 & 2\xi_{TMD}\omega_{TMD} & -2\xi_{TMD}\omega_{TMD} \end{bmatrix}$$

$$\mathbf{B} = [0 \quad 0 \quad -1/M_S \quad 1/\mu M_S]^T, \qquad \mathbf{H} = [0 \quad 0 \quad 1/M_S \quad 0]^T$$

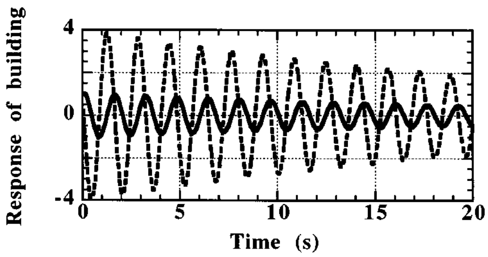

Figure 4. Uncontrolled response of SDOF model from initial conditions, (———, displacement (cm); – – – – – –, velocity (cm/s))

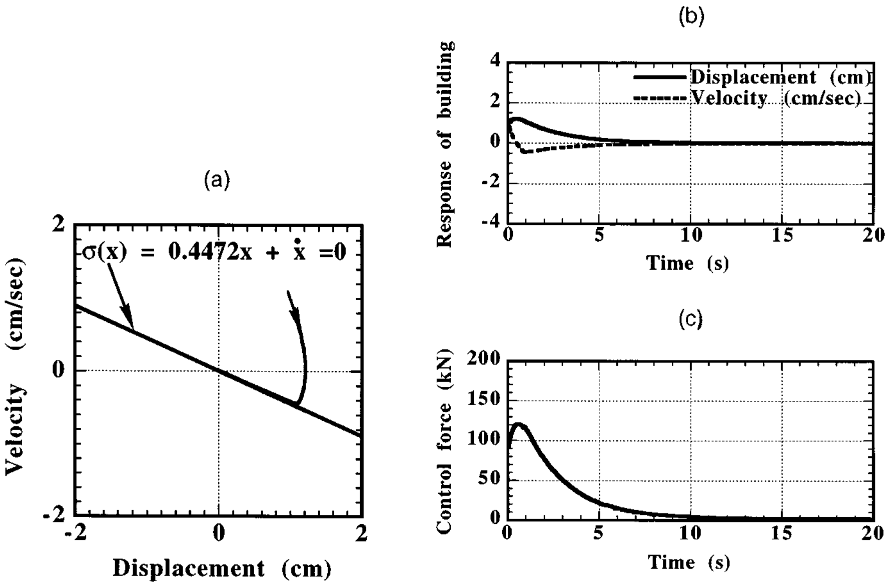

Figure 5. Response of SDOF model with force control for $\sigma(x) = 0.4472x + \dot{x}$ (no constraint on the control force): (a) phase plot; (b) response of the building; (c) control force

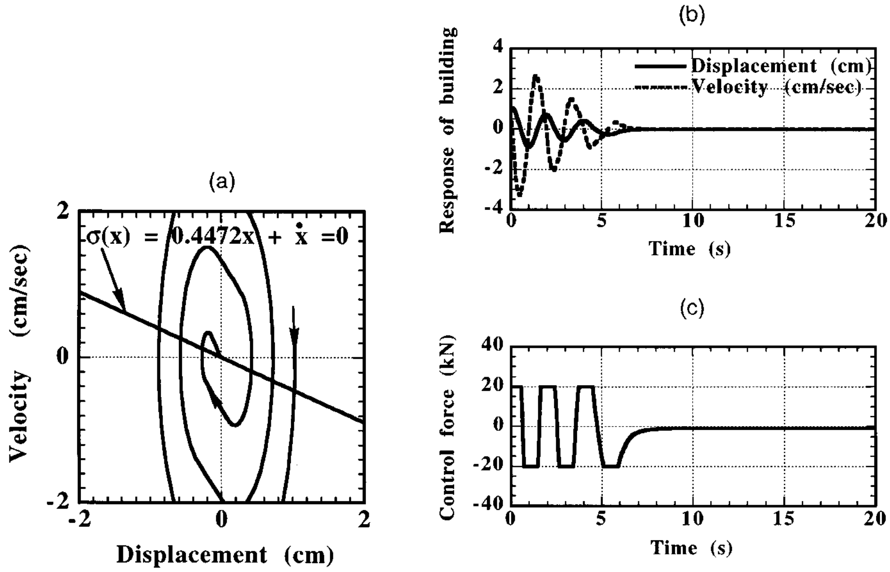

Figure 6. Response of SDOF model with force control for $\sigma(x) = 0.4472x + \dot{x}$ (constrained control force, $u_{MAX} = 20$ kN) : (a) phase plot; (b) response of the building; (c) control force

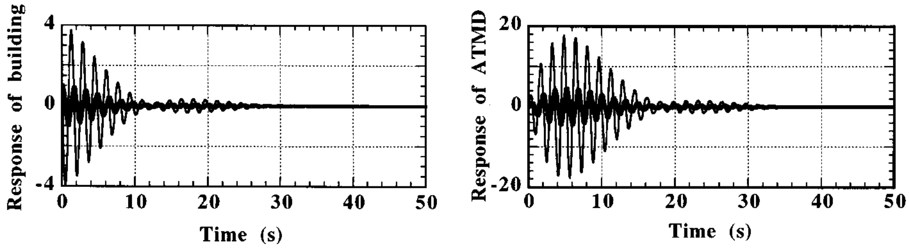

Figure 7. Response of the SDOF model of building–ATMD system from initial conditions, (———, displacement (cm); — — —, velocity (cm/s)

where μ, the mass ratio between the mass of the mass damper and the mass of the building, is assumed to be 0·01 (i.e. mass ratio of 1 per cent of the building mass M_s), M_s is taken to be equal to $698{\cdot}95 \times 10^3$ kg, ξ_{TMD} is assumed to be 6 percent, and ω_{TMD} is taken to be equal to the natural frequency of the structure ω_s. By following the same method as in Example 1(a), an optimal sliding surface was constructed as $\sigma(\mathbf{x}) = -113{\cdot}83x_s + 0{\cdot}95x_{TMD} + 2{\cdot}46\dot{x}_s + 1{\cdot}02\dot{x}_{TMD}$ for $Q = \mathrm{diag}[1000\ 1\ 1000\ 1]$.

The responses of the building–ATMD system from the initial condition of $\mathbf{x}(0) = [0{\cdot}01\ 0{\cdot}0\ \ 0{\cdot}01\ 0{\cdot}0]$, were obtained and are shown in Figure 7. The controlled response of the building–ATMD system for the same initial conditions with a maximum control force capacity of 20 kN is also shown in Figure 8. Here, η was selected to be a constant equal to 5 kN.

It is seen in Figures 8(a) and (c), that even with an optimally designed sliding surface, the building is not controlled effectively and that after some time from the start of the control action, the building response increases before being reduced again. The phase plot for the building responses, Figure 8(a), shows that the trajectories tend to diverge from the origin instead of being converged to it. In order to see the possible cause of this undesirable control performance, the response of the ATMD mass is plotted in Figures 8(b) and 8(d). Also plotted is the time history of control force in Figure 8(e). It is seen in Figures 8(c)–8(e), that even when the response of the structure itself is not significantly large, large displacement of the ATMD mass takes place and a large control force is applied on the building. This may be because as both the u_{eq} and $\sigma(\mathbf{x})$ are

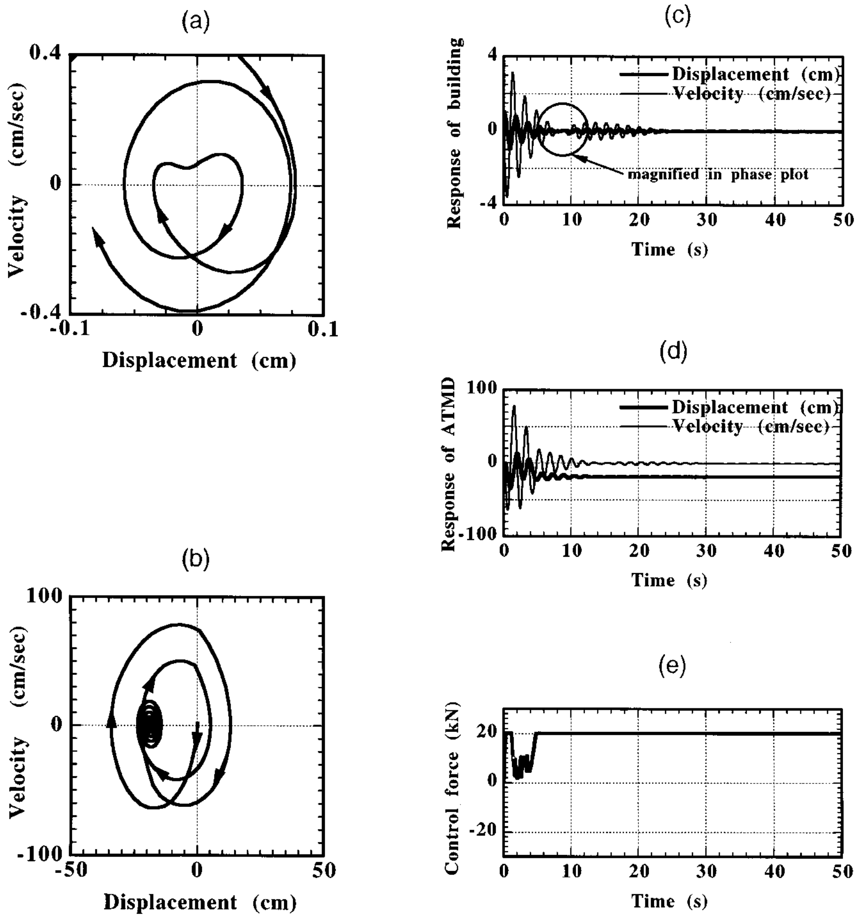

Figure 8. SMC controlled response of the SDOF model of building–ATMD system for $\sigma(x) = -113.83x_s + 0.95x_{TMD} + 2.46\dot{x}_s + 1.02\dot{x}_{TMD}$. (constrained control force, $u_{MAX} = 20$ kN) : (a) phase plot for the building plotted for 5–11.5 s of response; (b) phase plot for the ATMD; (c) response of the building; (d) response of the ATMD mass; (e) control force

functions of the building responses as well as the ATMD responses, the large values of the ATMD response, Figures 8(b) and 8(d), results in large values for u_{eq} which, in turn, excites the building instead of controlling it. Similarly, the large displacement of ATMD, Figure 8(d), prevents $\sigma(\mathbf{x})$ from approaching to zero and thereby causing a continued non-linear control action, which results in a large control force as seen in Figure 8(e). This continued non-linear action is undesirable as it causes large response in the controlled system. In other words, interaction between the ATMD and structure takes place which prevents the main control objective of maintaining the controlled system on the sliding surface.

Thus, it is seen that the direct application of the conventional sliding mode control concept to a tall building with an ATMD installed at the top may lead to large responses in the controlled building due to the interaction between the ATMD and the building.

SLIDING MODE CONTROL WITH COMPENSATOR FOR BUILDINGS WITH ATMD

Eliminating the effects of ATMD

One of the ways to eliminate the ATMD–building interaction would be to design SMC such that the sliding surface is independent of the ATMD response whereas the control force retains some of the

characteristics of the ATMD response. This would ensure that the building response is controlled and the ATMD responses are also minimized so that the stability of the ATMD system is maintained. Here, we propose to use a compensator and design the sliding surface based on the response of this compensator[20] instead of the state variables of the original ATMD–building system. This implies that the condition of satisfying the sliding mode conditions is related to the response of the compensator rather than those of the building.

Let the original ATMD–building system represented by equation (2) be transformed into a new co-ordinate system $\mathbf{y} = \mathbf{T}\mathbf{x}$, where $\mathbf{T}$ is a transformation matrix, such that the system in the transformed co-ordinates, neglecting the external excitation, is obtained as

$$\begin{bmatrix} \dot{\mathbf{y}}_1 \\ \dot{\mathbf{y}}_2 \end{bmatrix} = \begin{bmatrix} \mathbf{A}^*_{11} & \mathbf{A}^*_{12} \\ \mathbf{A}^*_{21} & \mathbf{A}^*_{22} \end{bmatrix} \begin{Bmatrix} \mathbf{y}_1 \\ \mathbf{y}_2 \end{Bmatrix} + \begin{bmatrix} \mathbf{0} \\ \mathbf{B}_2 \end{bmatrix} u \tag{9}$$

where $\mathbf{y}_1$ of size $(2n - r)$ and $\mathbf{y}_2$ of size r are obtained from $\mathbf{y} = \mathbf{T}\mathbf{x}$, and submatrices $\mathbf{A}^*_{ij}$ are the block matrices appearing in $\mathbf{T}\mathbf{A}\mathbf{T}^{-1}$. The system represented in the form of equation (9) is known as the regular form.[19] In the regular form, all the elements of $\mathbf{B}$, except a submatrix $\mathbf{B}_2$ of size $r \times r$ located at the bottom of $\mathbf{B}$, are zero.

Let the sliding surface now be defined as

$$\varphi(\mathbf{z}) = \mathscr{S}_1 z_1 + \mathscr{S}_2 z_2 \tag{10}$$

where $\mathbf{z}$ represents the compensator states realized through the following dynamical system which is also represented in the regular form:

$$\begin{bmatrix} \dot{z}_1 \\ \dot{z}_2 \end{bmatrix} = \begin{bmatrix} F_{11} & F_{12} \\ F_{21} & F_{22} \end{bmatrix} \begin{Bmatrix} z_1 \\ z_2 \end{Bmatrix} + \begin{bmatrix} \mathbf{G}_1 \\ \mathbf{G}_2 \end{bmatrix} \mathbf{y} + \begin{bmatrix} 0 \\ D_2 \end{bmatrix} u \tag{11}$$

Since, once the system is in the sliding mode, it satisfies $\varphi(\mathbf{z}) = 0$ and $\dot{\varphi}(\mathbf{z}) = 0$ and the control force is the so-called equivalent control,[11,16] the augmented system comprising the building and the compensator can be represented in the sliding mode as

$$\dot{\mathbf{y}}^* = \mathbf{A}^*\mathbf{y}^* + \mathbf{B}^*\mathbf{u}^* \tag{12}$$

where

$$\mathbf{y}^* = \begin{Bmatrix} \mathbf{y}_1 \\ \mathbf{y}_2 \\ z_1 \end{Bmatrix}, \qquad \mathbf{A}^* = \begin{bmatrix} \mathbf{A}^*_{11} & \mathbf{A}^*_{12} & \mathbf{0} \\ \mathbf{A}^*_{21} & \mathbf{A}^*_{22} & \mathbf{0} \\ \mathbf{0} & \mathbf{0} & 0 \end{bmatrix}, \qquad \mathbf{B}^* = \begin{bmatrix} \mathbf{0} & \mathbf{0} \\ \mathbf{B}_2 & \mathbf{0} \\ 0 & 1 \end{bmatrix}, \qquad \mathbf{u}^* = \begin{Bmatrix} u_{\mathrm{eq}} \\ \dot{z}_1 \end{Bmatrix} \tag{13}$$

It is clear that equation (12) represents a standard full state feedback control system for which the full state feedback control force can be obtained in the form of[20]

$$\mathbf{u}^* = -\mathbf{K}^*\mathbf{y}^* \tag{14}$$

where $\mathbf{K}^*$ is the so-called gain matrix.

Also, by satisfying the condition that $\varphi(\mathbf{z}) = 0$ and $\dot{\varphi}(\mathbf{z}) = 0$, it can be shown from equations (10) and (11) that

$$\mathbf{u}^* = \begin{bmatrix} -(\mathscr{S}_2 D_2)^{-1}(\mathscr{S}_1\mathbf{G}_1 + \mathscr{S}_2\mathbf{G}_2) & -(\mathscr{S}_2 D_2)^{-1}(\mathscr{S}_1 F^*_{11} + \mathscr{S}_2 F^*_{12}) \\ \mathbf{G}_1 & F^*_{11} \end{bmatrix} \mathbf{y}^* \tag{15}$$

where

$$\begin{aligned} F^*_{11} &= F_{11} - F_{12}\mathscr{S}_2^{-1}\mathscr{S}_1 \\ F^*_{12} &= F_{21} - F_{22}\mathscr{S}_2^{-1}\mathscr{S}_1 \end{aligned} \tag{16}$$

Thus, comparing equation (14) with equation (15), $\mathbf{K}^*$ is obtained to be

$$\mathbf{K}^* = -\begin{bmatrix} -(\mathscr{S}_2 D_2)^{-1}(\mathscr{S}_1\mathbf{G}_1 + \mathscr{S}_2\mathbf{G}_2) & -(\mathscr{S}_2 D_2)^{-1}(\mathscr{S}_1 F_{11}^* + \mathscr{S}_2 F_{12}^*) \\ \mathbf{G}_1 & F_{11}^* \end{bmatrix} \tag{17}$$

Hence, once the gain $\mathbf{K}^*$ of equation (14) is obtained by any of the standard methods, e.g. pole placement or LQ control theory, the design parameters for the compensator, i.e. $\mathbf{F}, \mathbf{G}$ and $\mathbf{D}$, can be obtained by comparing $\mathbf{K}^*$ of equation (14) with that of equation (17). In equation (17), $\mathscr{S}_1$ and $\mathscr{S}_2$ may either be selected arbitrarily or can be obtained by following the method of designing the optimal sliding surface as indicated earlier. $\mathbf{D}_2$ of equation (17) can be assumed to be the same as $\mathbf{B}_2$,[20] whereas F_{11} and F_{22} are selected arbitrarily with due care taken so that for any selected values of F_{11} and F_{22}, the resulting augmented system remains stable.

Here, we also point out that with a proper choice of the compensator parameters it is possible to manipulate the behaviour of the controlled system through response shaping. A strategy could also be to use the filtering feature of the compensator to filter out the unwanted high-frequency response caused by the non-linear switching control action involved in the sliding mode control. In other words, frequency shaping in the sliding mode response could be achieved by designing properly the compensator transfer function.[22] However, the problem then becomes a frequency domain problem which is beyond the scope of this paper and is not pursued here.

Design of the control force

Though the external excitation is generally neglected in the design of the compensator, it is included here for the design of the control force, so that the properties of the external excitations are included in the control law. The state equations for the compensator including the external excitation is written as

$$\begin{bmatrix} \dot{z}_1 \\ \dot{z}_2 \end{bmatrix} = \begin{bmatrix} F_{11} & F_{12} \\ F_{21} & F_{22} \end{bmatrix} \begin{Bmatrix} z_1 \\ z_2 \end{Bmatrix} + \begin{bmatrix} \mathbf{G}_1 \\ \mathbf{G}_2 \end{bmatrix} \mathbf{y} + \begin{bmatrix} 0 \\ D_2 \end{bmatrix} u + \begin{bmatrix} 0 \\ H_2^* \end{bmatrix} \mathbf{f}(t) \tag{18}$$

where H_2^* is a r-dimensional vector which represents the locations for the external excitation being applied at the locations of the controllers. H_2^* is obtained from $\mathbf{H}$ as a subset of $\mathbf{H}$ with elements corresponding to the locations of the controllers.

The expression for u_{eq} is then obtained by satisfying $\dot{\varphi}(\mathbf{z}) = 0$, as

$$u_{\text{eq}} = -(\mathscr{S}_2 D_2)^{-1}\left[(\mathscr{S}_1 G_1 + \mathscr{S}_2 G_2)\mathbf{y} + (\mathscr{S}_1 F_{11}^* + \mathscr{S}_2 F_{12}^*) z_1\right] \tag{19}$$

whereas the expression for the non-linear control action η is obtained by satisfying the conditions for the existence and reachability of the sliding motion, which is now expressed in terms of $\varphi(\mathbf{z})$ as $\varphi(\mathbf{z})\dot{\varphi}(\mathbf{z}) < 0$. η is derived to be given by

$$\eta(t) \geqslant |(\mathscr{S}_2 D_2)^{-1}\left[(\mathscr{S}_1 F_{12} + \mathscr{S}_2 F_{22})(\mathscr{S}_2^{-1}\mathscr{S}_1 z_1 + \dot{z}) + \mathscr{S}_2 H_2^* \hat{\mathbf{f}}(t)\right]| \tag{20}$$

It should be noted that following similar arguments as given before, the term containing $\mathbf{f}(t)$ has been neglected while obtaining the expression for u_{eq} in equation (19). It should also be noted here that the term relating to the non-linear control action $\eta(t)$ as given by equation (20), is a function of the states of the compensator as well as a function of the uncertainty in the system $\hat{\mathbf{f}}(t)$. Since the states of the compensator are nothing but a filtered version of the states of the system, the non-linear control action can be viewed as an implicit function of the states of the system also. As the non-linear control action imparts robustness to the control law, the robustness thus achieved is a function of both the states of the system and the uncertainty in the external excitation.

Numerical examples

The effectiveness of the sliding mode control scheme developed herein for the practical application of ATMD to control the vibration of a tall building is demonstrated in this section. For the purpose, the building is modelled as a SDOF system with an ATMD installed at the top of the building, as shown in Figure 3(b). The system matrices remain the same as in the case of Example 1(b). Assuming $F_{12} = -1{\cdot}0$, $F_{22} = -10{\cdot}0$ and $\mathscr{S} = [0{\cdot}4472\ \ 1]$, which is the same as the optimal sliding surface obtained for the SDOF model of the previous Example 1(a), the other parameters defining the compensator were obtained to be $F_{11} = 1{\cdot}45$, $F_{21} = -4{\cdot}02$, $\mathbf{G}_1 = [0\ 0\ 0\ 0]$, $\mathbf{G}_2 = [-1{\cdot}47 \times 10^2\ \ 6{\cdot}63 \times 10^{-5}\ \ 5{\cdot}72\ \ 1{\cdot}32]$, $D_1 = 0$ and $D_2 = -1{\cdot}43 \times 10^{-4}$. These values were obtained by minimizing a performance index $J = \int_0^\infty (\mathbf{y}^{*\mathrm{T}}\mathbf{Q}\mathbf{y}^* + \mathbf{u}^{*\mathrm{T}}\mathbf{R}\mathbf{u}^*)\,\mathrm{d}t$ to obtain $\mathbf{K}^*$ of equation (14) with $\mathbf{y}^* = [\mathbf{y}_1^{\mathrm{T}}\ \mathbf{y}_2^{\mathrm{T}}\ z_1^{\mathrm{T}}]$ and $\mathbf{u}^* = [u_{\mathrm{eq}}^{\mathrm{T}}\ z_1^{\mathrm{T}}]^{\mathrm{T}}$. The matrix $\mathbf{Q}$ was selected as $\mathbf{Q} = \mathrm{diag}[1000\ 1\ 1 \times 10^6\ 20\ 1]$ and the matrix $\mathbf{R}$ was selected as $\mathbf{R} = \mathrm{diag}[1 \times 10^{-5}\ \ 1]$.

(a) *Performance under initial condition excitation.* The response of the structure–ATMD system under the newly designed sliding mode control scheme is shown in Figure 9 for the initial conditions of $\mathbf{x}(0) = [0{\cdot}01\ 0{\cdot}0\ \ 0{\cdot}01\ 0{\cdot}0\ 0{\cdot}0\ 0{\cdot}0]$ which is the same as assumed in Example 1(b), except for the added terms corresponding to the compensator states. Here, η was calculated by using equation (20) in which $\hat{\mathbf{f}}(t)$ was

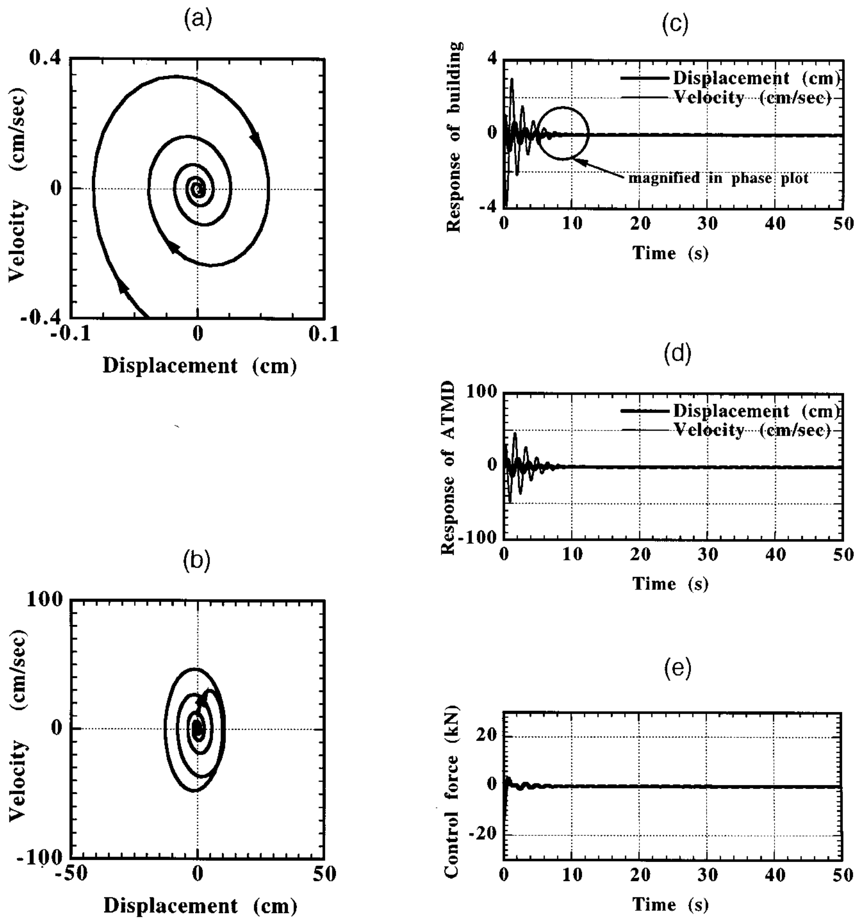

Figure 9. SMC controlled response of the SDOF model of building–ATMD system for $\varphi(z) = 0.4472z + \dot{z}$: (a) phase plot for the building; (b) phase plot for the ATMD; (c) response of the building; (d) response of the ATMD mass; (e) control force

neglected for the present case of vibration from initial conditions. It is seen in Figures 9(a)–9(d) that both the structure and the ATMD response are brought to rest as a well-behaved damped system. The interaction effect is completely removed. The time history of the responses of the building as well as that of the ATMD indicates that the control objective is completely accomplished. Thus, it can be concluded here that the design of a compensator, which acts as a filter in the sliding surface, can remove the interaction effect from the ATMD responses onto the structure, and thus prevents the possibility of large responses in the controlled system. It is also seen in Figure 9 that not only the response of the building is effectively controlled, but the response of the ATMD is also not very large and a considerably smaller control force is required as compared to the control force required for the case of control without the compensator, Figure 8.

(b) *Performance under external excitation.* The performance of the structure–ATMD system under the newly designed sliding mode control scheme is next discussed under the condition of two different external excitations. The external excitations chosen here are the wind forces acting on the structure. The time histories of the wind forces estimated from the recorded time histories of the wind velocity are shown in Figure 10. Also shown in the same figure is the time series of the estimated uncertainty in the wind force. The uncertainty in the wind loading represented by $\hat{\mathbf{f}}(t)$ of equation (20), was assessed by computing the variation in the energy of wind turbulence and then relating it to the theory of steady-state aerodynamics.[18, 23] Though, ideally, it is desirable to change η with changes in the external excitation, frequent changes in η may not be practically feasible. Therefore, wind in this case is treated to be a piecewise stationary process within a time interval of T, and η is assumed to be constant during this time interval. The uncertainty in the wind forces within T, now represented by $\hat{\mathbf{f}}(T)$, was obtained as

$$\hat{\mathbf{f}}(T) \approx \tfrac{1}{2}\,\rho C_{\mathrm{D}} B(2U_{\mathrm{EQ}}(T)\, u_{\mathrm{RMSeq}}(T) + u^2_{\mathrm{RMSeq}}(T)) \tag{21}$$

where ρ is the density of air, C_{D} is the coefficient of wind drag, B is the dimension of the structure perpendicular to the wind flow and T is the averaging time used for the evaluation of the mean wind velocity. $U_{\mathrm{EQ}}(T)$ and $U_{\mathrm{RMSeq}}(T)$ are defined as the equivalent mean wind velocity and root mean square of its fluctuating components, respectively, that would give rise to a certain amount of variation in the wind energy of turbulence in excess of its mean energy evaluated for a time interval of T. For all of the simulations to follow, T is taken to be 1 min and $\eta(t)$ is replaced by $\eta(T)$.

The parameters related to the compensator, e.g. the values of $\mathbf{F}$ and $\mathbf{D}$ were selected to be the same as that of the previous case. However, $\mathbf{G}$ for this case of external excitation was selected to be $G_1 = [0{\cdot}0\;\; 0{\cdot}0\; 0{\cdot}0\; 0{\cdot}0]$ and $G_2 = [-209{\cdot}1423\;\; 0{\cdot}0131\;\; 6{\cdot}0446\;\; 3{\cdot}0783]$, whereas $\mathscr{S}$ was assumed to be the same as in the previous case of force control of the SDOF model, i.e. $\mathscr{S} = [0{\cdot}4472\;\; 1]$. The value of $\eta(T)$ was calculated by using equation (20) in which t is replaced by T, and $\hat{\mathbf{f}}(T)$ was obtained from equation (21).

The simulation results for uncontrolled and the controlled responses for cases with and without compensator are shown together in Figures 11 and 12. Figure 11 depicts the phase plots of the response of the building, whereas Figure 12 depicts the phase plots of the response of the ATMD mass. Comparing

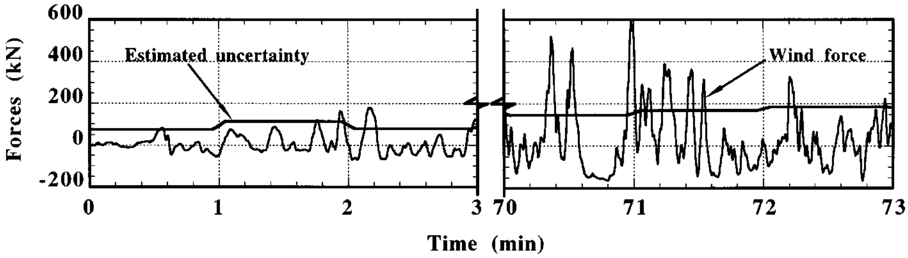

Figure 10. Time series of the estimated wind force and the estimated uncertainty in the wind force

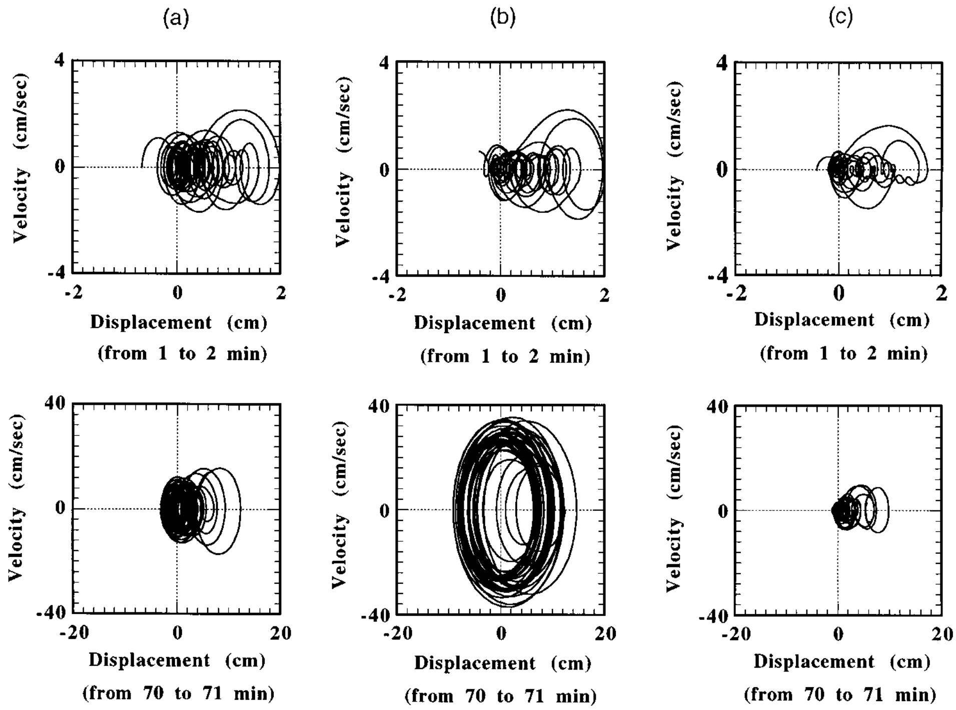

Figure 11. Phase plots of the response of the SDOF model of the building with ATMD for: (a) uncontrolled case; (b) control without compensator and; (c) control with compensator

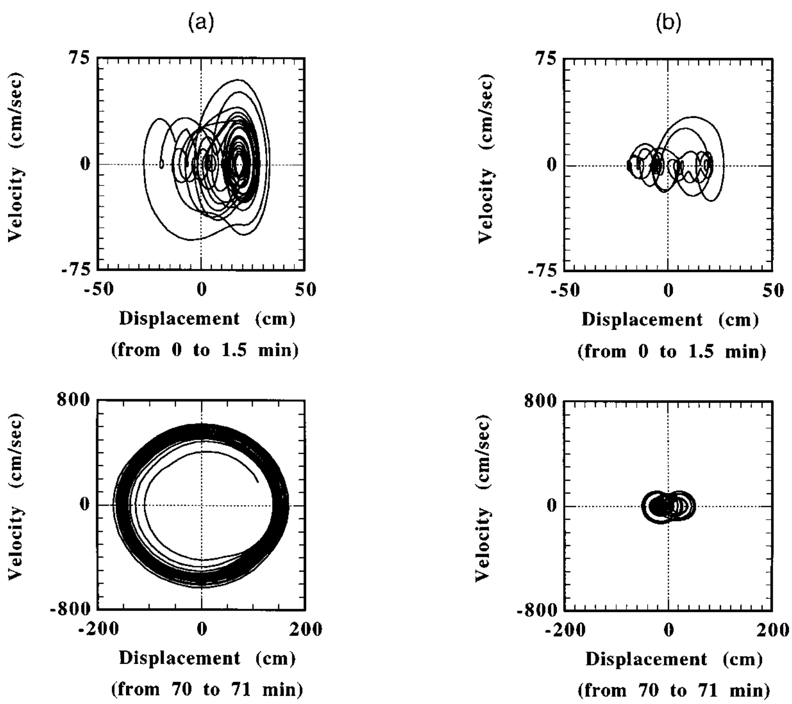

Figure 12. Phase plots of the response of the ATMD for (a) control without compensator and (b) control with compensator

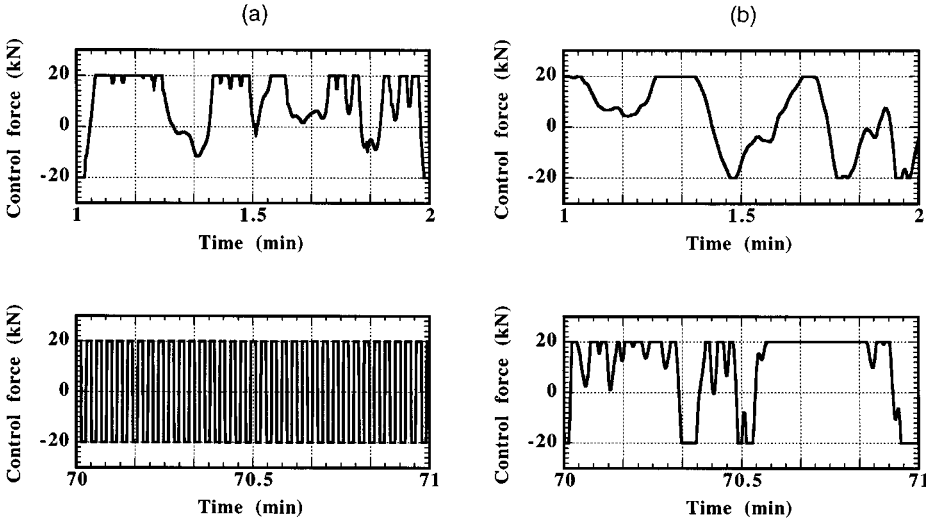

Figure 13. Control force for control: (a) without compensator and; (b) with compensator

Figure 11(b) with Figure 11(a), it is seen that the controlled response for the case of control without compensator for the first 1–2 min is slightly reduced. However, when the external excitation is quite large, as is in the case of 70–71 min, the performance of the control without compensator degrades considerably. This is because the sliding surface in this case is constructed taking into account of the degrees of freedom of the ATMD also, and the control force is based on the state vector and the sliding surface matrix **S** (equation (5)). Therefore, the considerably large response of the ATMD, as shown in Figure 12(a), results in a large control force which in turn excites the building instead of controlling it. This situation, obviously, is highly undesirable. However, as it is seen in Figure 11(c), the control performance for the case of control with compensator is considerably improved.

Figures 11 and 12 show that the control with compensator not only reduces the response of the building but it reduces the response of the ATMD also. This can be explained by examining the control force, shown in Figure 13. Figure 13 shows that the control without a compensator results in a high controller activity which is due to the large response of the ATMD. The control force in this case is utilized to keep the ATMD mass moving instead of controlling the building response. This further increases the response of the ATMD thus resulting in a larger ATMD response in Figure 12(a). This also results in increased building response, as shown in Figure 11(b). However, when the control is applied through the compensator, the undesirable effect of the ATMD on the control performance is minimized. This results in improved control performance by reducing the response of the building as well as that of the ATMD.

Note that all of the phase plots of Figure 11 show an inclination towards the positive displacement, which is due to the very low-frequency displacement caused by the slowly varying mean wind velocity.

CONCLUDING REMARKS

In the present paper, the problem associated with the application of sliding mode control algorithm for the control of a tall building with ATMD as a control device has been addressed and resolved. It is shown that the direct application of the conventional sliding mode control theory may cause large response in the building due to the interaction effect between ATMD and the building arising because of the large responses of the ATMD. In order to rectify this problem, a filter has been proposed and designed so that the influence of

the ATMD responses on the control forces as well as on the sliding surface can be eliminated by filtering out responses. It has been shown through simulation results of the building–ATMD system subjected to two different external excitations, that the application of such a filter on the sliding surface helps reduce the interaction effect from the ATMD onto the structure. Here, it is worth mentioning that the problem caused by the comparatively large response of the ATMD could probably be eliminated by some other methods also, e.g. by choosing a very appropriate sliding surface by doing a number of trials and errors with various optimal sliding surfaces. But that would result in a more tiresome and time-consuming design process. Instead, a better performance with ATMD under SMC platform can be obtained by designing appropriately a filter to eliminate the undesirable effects of the ATMD.

REFERENCES

1. J. Roorda, 'Tendon control in tall structures', *J. struct. div. ASCE* **101**, 505–521 (1975).
2. J. N. Yang and F. Giannopoulos, 'Active tendon control of structures', *J. eng. mech. div. ASCE* **104**, 551–568 (1978).
3. J. N. Yang and M. J. Lin, 'Building critical-mode control: nonstationary earthquake', *J. eng. mech. div. ASCE* **109**, 1375–1389 (1982).
4. T. T. Soong and G. T. Skinner, 'Experimental study of active structure control', *J. eng. mech. div. ASCE* **107**, 1057–1068 (1981).
5. J. C. H. Chang and T. T. Soong, 'Structural control using active tuned mass damper', *J. eng. mech. ASCE* **106**, 1091–1098 (1980).
6. M. Abdel-Rohman, 'Optimal design of active TMD for building control', *Building environ.* **19**, 191–195 (1984).
7. T. Kobori, N. Koshika, K. Yamada and Y. Ikeda, 'Seismic-response-controlled structures with active mass driver system. Part 1: design', *Earthquake eng. struct. dyn.* **20**, 133–149 (1991).
8. T. Kobori, N. Koshika, K. Yamada and Y. Ikeda, 'Seismic-response-controlled structures with active mass driver system. Part 2: verification', *Earthquake eng. struct. dyn.* **20**, 151–166 (1991).
9. B. K. Bhartia, Y. Fujino and J. Mongkol, 'On linear-saturation (LS) control of buildings', *Earthquake eng. struct. dyn.* (1994) (submitted).
10. V. I. Utkin, 'Variable structure systems with sliding modes', *IEEE trans. automat. control* **AC22**, 212–222 (1977).
11. V. I. Utkin, 'Variable structure systems-present and future', *Automation remote control* **44**, 1105–1120 (1983).
12. J.-J. E. Slotine and J. A. Coetsee, 'Adaptive controller synthesis for nonlinear systems', *Int. j. control* **43**, 1631–1651 (1986).
13. J.-J. E. Slotine and W. Li, *Applied Nonlinear Control*, Prentice-Hall, Englewood Cliffs, NJ, 1991.
14. O. M. E. El-Ghezawi, A. S. Zinober and S. A. Billings, 'Analysis and design of variable structure systems using a geometric approach', *Int. j. control* **38**, 657–671 (1983).
15. R. A. DeCarlo, S. H. Zak and G. P. Matthews, 'Variable structure control of nonlinear multivariable systems: a tutorial', *Proc. IEEE* **76**, 212–232 (1988).
16. B. Draženovic, 'The invariance conditions in variable structure systems', *Automatica* **5**, 287–295 (1969).
17. J. N. Yang J. C. Wu, A. K. Agrawal and Z. Li, 'Sliding mode control for seismic-excited linear and nonlinear civil engineering structures', *Technical Report, NCEER-94-0017*, 1994.
18. R. Adhikari and H. Yamaguchi, 'Robust-adaptive control of wind-induced vibration of tall buildings', *J. eng. mech. div. ASCE* (1995) (submitted).
19. V. I. Utkin and K. D. Young, 'Methods for constructing discontinuous planes in multidimensional variable structure systems', *Automation remote control* **31**, 1466–1470 (1978).
20. B. Friedland, *Control System Design: An Introduction to State–Space Methods*, 2nd edn., McGraw-Hill, New York, 1987.
21. E. P. Ryan, 'A variable structure approach to feedback regulation of uncertain dynamical systems', *Int. j. control* **38**, 1121–1134 (1983).
22. K. D. Young and U. Özguner, 'Frequency shaping compensator design for sliding mode', *Int. j. control* **57**, 1005–1019 (1993).
23. R. Adhikari and H. Yamaguchi, 'Characterization of wind-induced gust response by Wavelets', (1996) (under preparation).

